Applied Catalysis A: General 374 (2010) 31–40

Contents lists available at ScienceDirect

Applied Catalysis A: General

journal homepage: www.elsevier.com/locate/apcata

# Hydroisomerization of *n*-decane over Ni–Pt–W supported on amorphous silica–alumina catalysts

Yacine Rezgui *, Miloud Guemini

*Laboratoire de Recherche de Chimie Appliquée et Technologie des Matériaux, Department of Chemistry, Université d'Oum El Bouaghi, B.P. 358, Route de Constantine, Oum El Bouaghi 04000, Algeria*

ARTICLE INFO

*Article history:*
Received 22 August 2009
Received in revised form 14 November 2009
Accepted 16 November 2009
Available online 20 November 2009

*Keywords:*
Platinum
Nickel
Isomerization
Cracking
*n*-Decane
Stability

ABSTRACT

A series of NiPtW/silica–alumina catalysts (wt.%: Ni, 12–17; W: 10, Pt: 0.1–1) were prepared via a hybrid method: sol–gel and incipient wetness impregnation and characterized by inductively coupled plasma-atomic emission spectroscopy (ICP-AES), BET, temperature-programmed desorption of ammonia ($NH_3$-TPD), pyridine adsorption followed by FTIR and TPO techniques. On these catalysts, *n*-decane hydroisomerization was carried out under the following conditions: fixed bed reactor, atmospheric pressure, temperature ranging from 150 to 300 °C, weight hourly space velocity of 4 $h^{-1}$ and molar hydrogen/hydrocarbon ratio of 5. Pt was found to promote activity and stability, the effect being optimal for 0.2 wt.% Pt. Isomers and cracking products yields were a function of both metal (Ni and Pt) content and conversion. Whatever *n*-decane conversion, monobranched isomers were found to be predominant. Besides, up to 10% conversion, the cracked products were not produced in significant amounts. For a time on stream of 100 min, the best results (47% conversion and 56% isomerization selectivity) were obtained at 250 °C over the catalyst containing 12% Ni, 10% W and 0.2% Pt).



## 1. Introduction

In the next few years lubricating oils will be used under increasingly severe conditions [1] and consequently oil refiners will be faced with many challenges. These include the production of lubes and middle-distillate fuels with advanced performance and environmental benefits. To fit in this situation, lubricants producers appeal to catalytic dewaxing process, which is used to remove hydrocarbons that have high freezing point, i.e., long-chain *n*-paraffins and to decrease the pour points of lubricating base stocks. These tasks are carried out chiefly by selective cracking of normal alkanes to lower the amount of molecular weight products which are later removed from the lube by normal distillation [2–5]. However, many studies have revealed that such a process gives low yields and mediocre properties of the dewaxed lube [5–7]. In order to improve the performance of the catalytic dewaxing procedure, attempts have recently been made to isomerize normal alkanes to isoalkanes, allowing them to remain in the oils and to produce higher quality oil in higher yield [8–13]. For this purpose, hydroisomerization and selective hydrocracking of long-chain normal paraffins have been intensely studied [14–16] and the difficulty of achieving high isomerization activity has been pointed out [17–19]. Thus the development of efficient catalysts for skeletal branching of long *n*-alkanes without cracking is a scientific challenge. Nowadays efforts have been made by industrial and academic researchers [20–22] to obtain solid acid catalysts which meet this task. In this context, Claude et al. [23] have mentioned that catalysts on which the highest yields of skeletal isomers from model long *n*-alkanes were obtained are molybdenum oxycarbides and noble metal loaded acid zeolites having uniform tubular pores with diameters of about 0.5 nm. On the other hand, Miller [24], Campelo et al. [25], Mériaudeau et al. [26], Sinha et al. [27] and Wanga et al. [28] have mentioned that SAPO-11 molecular sieves loaded with Pt or Pd exhibited high hydroisomerization selectivities. Besides, our previous investigations have reported that Ni–$WO_x$ supported on silica alumina catalysts can exhibit an interesting behavior in catalytic dewaxing if the rate of hydrogenolysis can be diminished [29]. To enhance the selectivity of Ni–$WO_x$ based catalysts to isomerization, platinum was incorporated. Previous investigations have reported the high catalytic activity of Ni–W–Pt supported on amorphous silica–alumina catalysts for hydrocarbon conversion at mild conditions [30]. Fairly high yields of branched isomers have been obtained using these catalysts for the isomerization of $C_6$ normal paraffins.

In this study, we focus on an analysis of the catalytic properties of a new type of catalysts Ni–Pt–W/$SiO_2$–$Al_2O_3$ for *n*-decane isomerization. We mainly discuss the role of metallic function content and the effect of process variables, like reaction time on stream, temperature, $H_2$/*n*-hydrocarbon molar ratio, and space velocity which can influence catalyst activity and selectivity.

* Corresponding author. Tel.: +213 63 12 71 62.
*E-mail address:* yacinereference@yahoo.com (Y. Rezgui).

0926-860X/$ – see front matter © 2009 Elsevier B.V. All rights reserved.
doi:10.1016/j.apcata.2009.11.021

## 2. Experimental

### 2.1. Catalyst preparation

The details of the preparation, by a hybrid method: sol–gel and incipient wetness impregnation, of a series of Ni–Pt–$WO_x$/$SiO_2$–$Al_2O_3$ catalysts, noted "$(Ni_xPt_y)_{AC}$" (where $x$ and $y$ indicate the percentage of nickel and platinum in the catalyst, while AC indicate that the incorporation of Pt was done after calcination), having the same amount of tungsten (10%) and a constant $SiO_2/Al_2O_3$ ratio (1.83), have been previously reported [31]. In brief:

A sol was obtained by mixing, under vigorous stirring, an aqueous solution of nickel nitrate ($Ni(NO_3)_2{\cdot}6H_2O$) preliminarily acidified by nitric acid with the required amounts of aluminum sulfate ($Al_2(SO_4)_3{\cdot}18H_2O$) and sodium tungstate ($Na_2WO_4$). To the obtained sol, an aqueous solution of sodium silicate ($Na_2SiO_3$) was added under vigorous stirring. To exchange undesirable ions, such as $Na^+$, the prepared gel was activated, under reflux conditions in a thermostat, with ammonium sulfate (liquid to solid ratio of 30) at 60 °C over a period of 48 h (this unit operation was repeated several times), washed with hot water (60 °C), dried at 120 °C for 4 h and finally calcined in the temperature range 300–700 °C for 5 h. A heating rate of 10 °C/min was used. The obtained solids were calcined at 500 °C for 5 h and then impregnated with a solution of hexachloroplatinic acid containing the appropriate concentration of Pt, the time of impregnation was 6 h. The samples thus prepared were dried at 120 °C overnight and calcined in the temperature range 300–700 °C for 5 h. A heating rate of 10 °C/min was used.

For comparison purposes, Pt-free catalysts containing 12%, 15%, 17% Ni and 10% of tungsten supported on amorphous silica–alumina were prepared as described in [32].

### 2.2. Catalysts characterization

Tungsten, nickel and platinum concentrations were measured by inductively coupled plasma-atomic emission spectroscopy (ICP-AES).

The acid-strength distribution of the prepared catalysts was measured by temperature-programmed desorption of ammonia ($NH_3$-TPD). All the catalysts were treated in situ in an oxygen flow at 500 °C for 3 h and then outgassed in helium flow at 300 °C. After reducing each catalyst under a hydrogen flow at its optimal reduction temperature (for more details see Ref. [31]) for 2 h, the sample was further dried in flowing He at 300 °C for 1 h and then cooled to room temperature. When the system become steady, the sample was saturated at 100 °C for 30 min in an ammonia stream (10% $NH_3$/He carrier gas) and then it was allowed to equilibrate in a helium flow at the same temperature for 1 h to remove the excess and physically adsorbed $NH_3$. The TPD spectrum was obtained by heating the sample from 100 to 700 °C at a heating rate of 10 °C/min under a He flow. Temperature and detector signals were simultaneously recorded. The area under the curve was integrated to determine the relative total acidity of the catalyst. For each sample, two peaks of ammonia desorption were observed, low desorption temperature (ranging from 150 to 220 °C reflecting the number of the weak acid sites) and high desorption temperature (ranging from 300 to 315 °C reflecting the amount of medium acid sites). In order to obtain the strength distribution, the desorption profiles were fitted using the two peaks, their maxima and widths being held as constant as possible while fitting each profile. The average relative error in the acidity determination was lower than 3%.

The nature of the acid sites was determined by Fourier infrared (FTIR) experiments. These experiments were done on a 170-SX Nicolet FTIR spectrometer. The sample was finely grounded and pressed into self-supporting wafer (14 mg/cm$^2$) and then placed in a heatable glass cell equipped with KBr windows, which permitted us to follow the changes of the spectrum with thermal treatments. Prior to IR measurements, each sample was treated in situ (in the cell) with a hydrogen flow at a specific temperature (optimal reduction temperature for each sample) for 2 h, evacuated to 0.1 Pa at the same temperature for 1 h, and then exposed to pyridine (1 Torr) at 100 °C for 20 min, outgassed 1 h at room temperature (pressure 0.1 Pa), and then heated up to the desired temperature using a linear program. The quantitative calculation of Lewis and Brönsted acid sites was made with respect to the integrated area of the adsorption bands at 1450 and 1540 cm$^{-1}$, respectively.

The amount and nature of the coke deposited on the catalysts at the end of the catalytic tests were determined by means of temperature-programmed oxidation. TPO measurements were carried out by passing a continuous flow of 5% $O_2$/He over catalysts as the temperature was increased linearly at 12 °C/min to 750 °C. Coke deposits were burned and the combustion gases converted to methane in a methanator by mixing the effluent with 0.83 cm$^3$ s$^{-1}$ $H_2$ and passing over a 15% $Ni/Al_2O_3$ catalyst held at 673 K. $CH_4$ formation rates were measured by a flame ionization detector, calibrated with 100 μl pulses of $CO_2$ and by the combustion of known amounts of graphite.

### 2.3. Catalyst activity measurements

All the catalysts prepared were tested for their activity and selectivity in hydroisomerization of $n$-decane in a continuous fixed-bed downflow quartz reactor, with a hydrogen and $n$-decane ($H_2/n$-$C_{10}$) molar ratio of 5, and a weight hourly space velocity (WHSV) of 4 h$^{-1}$. The reaction was performed at atmospheric pressure and a temperature ranging from 150 to 300 °C with a step of 50 °C. Prior to the reaction, the catalysts were reduced in situ in a hydrogen stream at their optimal reduction temperature for 3 h in order to prereduce the metallic function (the optimum reduction

**Table 1**
Physico-chemical properties of the $(Ni_xPt_y)_{AC}$ samples.

| Catalyst | % Ni | % Pt | % W | Optimum reduction temperature (°C) | Acid amount (mmol $NH_3$/g) | | Nature of acidity (μmol of pyridine/g) | |
|---|---|---|---|---|---|---|---|---|
| | | | | | Weak acidity | Medium acidity | Brönsted acidity (Br) | Lewis acidity (Le) |
| $(Ni_{12}Pt_0)$ | 12 | 0.0 | 10 | 420 | 0.13 | 0.11 | 52 | 121 |
| $(Ni_{12}Pt_{0.1})_{AC}$ | 12 | 0.1 | 10 | 400 | 0.16 | 0.08 | 95 | 77 |
| $(Ni_{12}Pt_{0.4})_{AC}$ | 12 | 0.4 | 10 | 410 | 0.18 | 0.06 | 96 | 77 |
| $(Ni_{12}Pt_1)_{AC}$ | 12 | 1.0 | 10 | 418 | 0.09 | 0.15 | 95 | 76 |
| $(Ni_{15}Pt_0)$ | 15 | 0.0 | 10 | 410 | 0.19 | 0.11 | 102 | 100 |
| $(Ni_{15}Pt_{0.1})_{AC}$ | 15 | 0.1 | 10 | 370 | 0.23 | 0.07 | 124 | 77 |
| $(Ni_{15}Pt_{0.4})_{AC}$ | 15 | 0.4 | 10 | 390 | 0.25 | 0.05 | 124 | 78 |
| $(Ni_{15}Pt_1)_{AC}$ | 15 | 1.0 | 10 | 404 | 0.27 | 0.03 | 123 | 77 |
| $(Ni_{17}Pt_0)$ | 17 | 0.0 | 10 | 425 | 0.10 | 0.26 | 130 | 89 |
| $(Ni_{17}Pt_{0.1})_{AC}$ | 17 | 0.1 | 10 | 365 | 0.12 | 0.24 | 140 | 78 |
| $(Ni_{17}Pt_{0.4})_{AC}$ | 17 | 0.4 | 10 | 395 | 0.13 | 0.23 | 141 | 78 |
| $(Ni_{17}Pt_1)_{AC}$ | 17 | 1.0 | 10 | 405 | 0.14 | 0.22 | 140 | 79 |

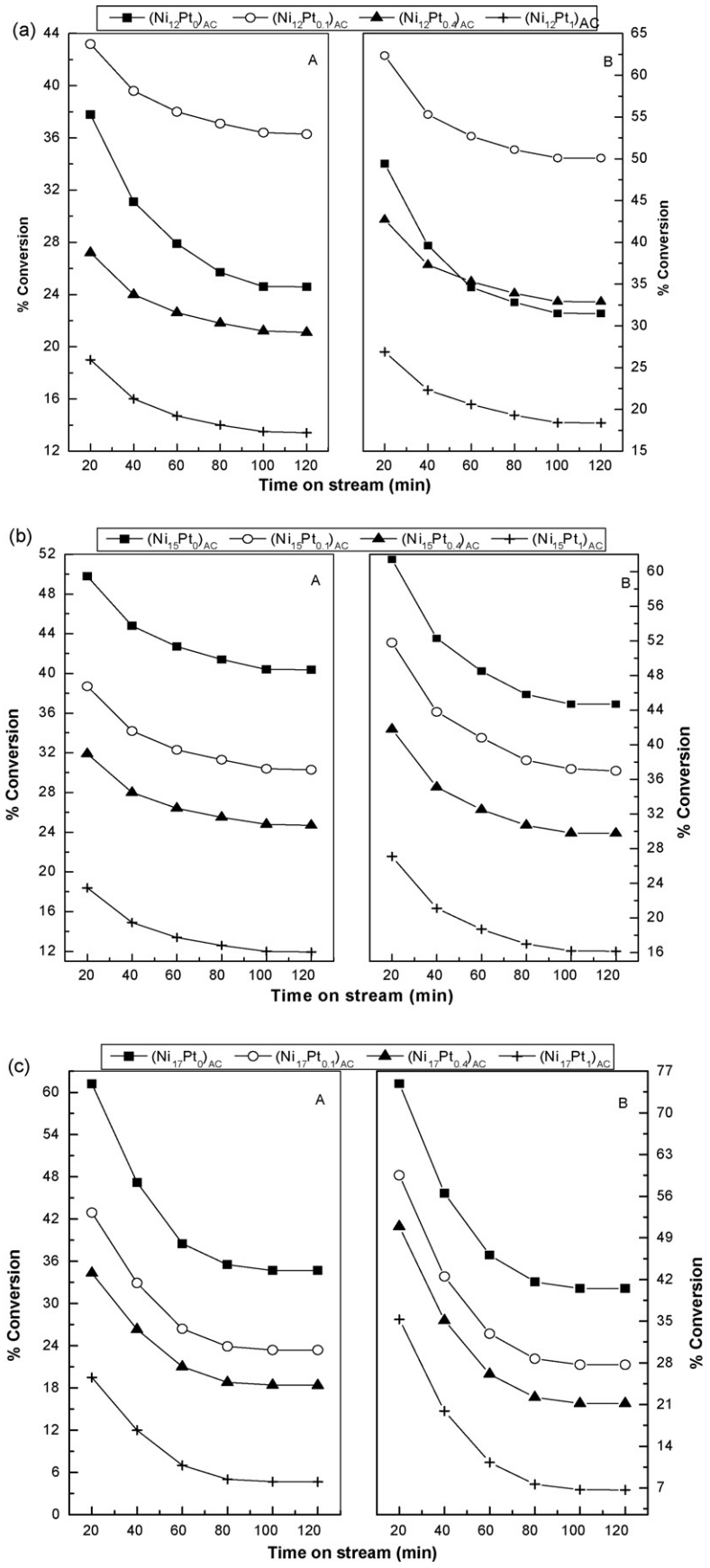


**Fig. 1.** (a) Evolution of $(Ni_{12}Pt_y)_{AC}$ catalysts activity with time on stream. (A) Reaction temperature = 150 °C and (B) reaction temperature = 300 °C. (b) Evolution of $(Ni_{15}Pt_y)_{AC}$ catalysts activity with time on stream. (A) Reaction temperature = 150 °C and (B) reaction temperature = 300 °C. (c) Evolution of $(Ni_{17}Pt_y)_{AC}$ catalysts activity with time on stream. (A) Reaction temperature = 150 °C and (B) reaction temperature = 300 °C.

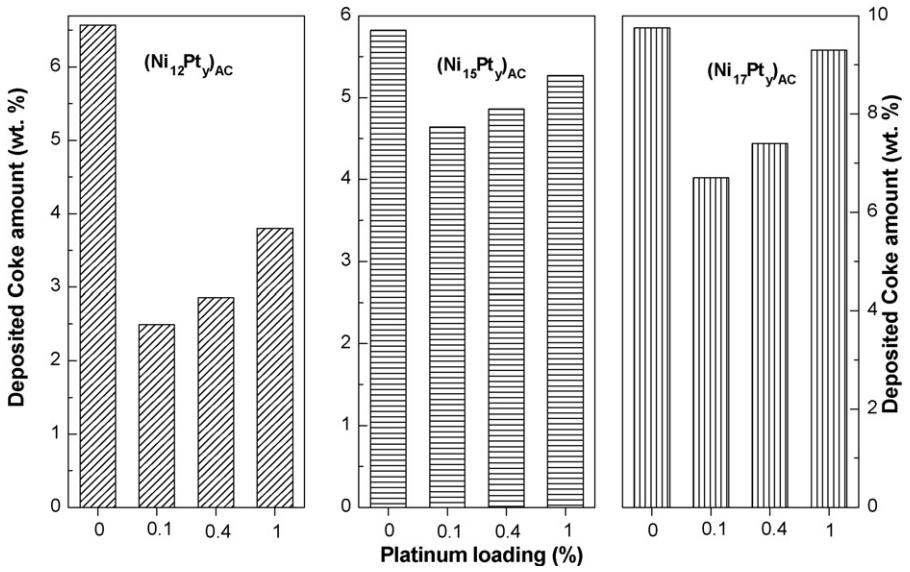


**Fig. 2.** Effect of the platinum loading on the amount of deposited coke over $Ni_xPt_y$ catalysts. Reaction conditions: reaction temperature 250 °C; time on stream (TOS) = 100 min.

temperature, for each prepared solid, is the temperature at which the three oxides (PtO, $WO_3$ and NiO) are reduced for this solid. For more details see Table 1 and the reference [31]). Then, the temperature was decreased to the desired reaction temperature. The products were analyzed using an on-line gas chromatograph.

Catalytic activity is expressed in term of conversion, which is defined as the fraction of the decane which has reacted. Selectivity was calculated by dividing the *i*-$C_{10}$ percentage in the products by *n*-$C_{10}$ conversion.

## 3. Results and discussion

### 3.1. Physico-chemical properties

Characterization parameters of the prepared catalysts are listed in Table 1. Weak, medium as well as Brönsted and Lewis acidities are shown. As can be clearly seen from the collected data, in the case of solids without platinum, an increase of nickel amount implies an increase of the number of the weak acid sites, which passed through a maximum at 15% of Ni and then decreased. Besides, increasing the nickel loading induces a rise in the amount of medium acid sites. Furthermore, the effect of Pt incorporation on the both type of acidities is dependent on the Ni amount; for solids with 12 wt.% Ni, the weak acidity increased, passed through a maximum at 0.4% of Pt then decreased, while in the case of 15 and 17 wt.% Ni catalysts, the Pt addition induced an enhancement in the density of weak acidity. Opposite trends were observed for the medium acidity. On the other hand, regardless the nickel content, the incorporation of 0.1 wt.% of platinum induced a large increase in Brönsted acid sites at the expense of Lewis acidity while maintaining the density of total sites constant; the phenomenon being more noticeable at lower nickel loadings. A further increase in platinum amount does not practically affect the nature of the catalysts acidity.

### 3.2. Catalytic stability and coke formation

The effect of time on stream was studied at the catalysts optimum reduction temperature using the above-mentioned operating conditions. During the catalytic transformation of *n*-decane, the conversion decreased gradually with time on stream (Fig. 1a–c) before reaching a steady state at about 100 min. This decrease, due to catalysts deactivation, was more drastic during the first few minutes. The deactivation rate was also more rapid at higher temperatures (Fig. 1a–c (B)). It is noteworthy that the deactivation rates were higher for catalysts without platinum compared to the promoted ones, suggesting that the Pt particles on the support play an important role in keeping the surface free from coke, same results were reported by Grau et al. [33] during their study on the isomerization-cracking of *n*-octane and *n*-decane over $Pt/WO_x–SO_4–ZrO_2$ catalysts. On the other hand, the collected data suggest that the deactivation rate depends directly upon the density of medium acid sites. In this mean, the higher the medium acid sites concentration, the higher the deactivation rate (comparison of the stability of the solids with 17% Ni, having the higher medium acidity from 0.24 to 0.28 mmol $NH_3$/g, with the samples with 12% Ni, having the lowest medium acid sites concentration from 0.11 to 0.15 mmol $NH_3$/g). The same results were reported by our group [31] during the study of the isomerization of *n*-hexane over the same catalysts. In summary, it can be considered that the catalysts stability is related to the density of acid sites and to the nickel and platinum contents, which means that the deactivation may be due to a metallic function poisoning, or to a loss of the support acidity, or finally, to a loss of the hydrogen dissociation capacity of $WO_x$ species, which is rapidly deactivated by coke [34].

To elucidate the role of platinum in enhancing the catalysts stability, coke formed on the prepared solids, during the hydroconversion of *n*-decane, was studied by TPO. The TPO spectra (figure not shown) indicated that an overall decrease of the TPO areas was observed as 0.1 wt.% of platinum was incorporated; the effect was more noticeable for solids with 12% Ni. However a further increase in the Pt amount induced a rise in the intensity of the peaks and a shift in their positions toward high temperature values. These effects and the results of deposited coke amounts depicted in Fig. 2, suggest that in the range 0.1–1 wt.% Pt, greater amounts of coke and more graphitic structures were obtained. However, for the same nickel loading, the area of the much intense peak and the value of its position, in the case of platinum promoted catalysts, were lower than those obtained for unpromoted solids which means that that the fist samples displayed much less deposited coke amount as well as much less graphitic coke than the latter ones. From these results and FTIR measurements, we can speculate that platinum helps to minimize deactivation resulting

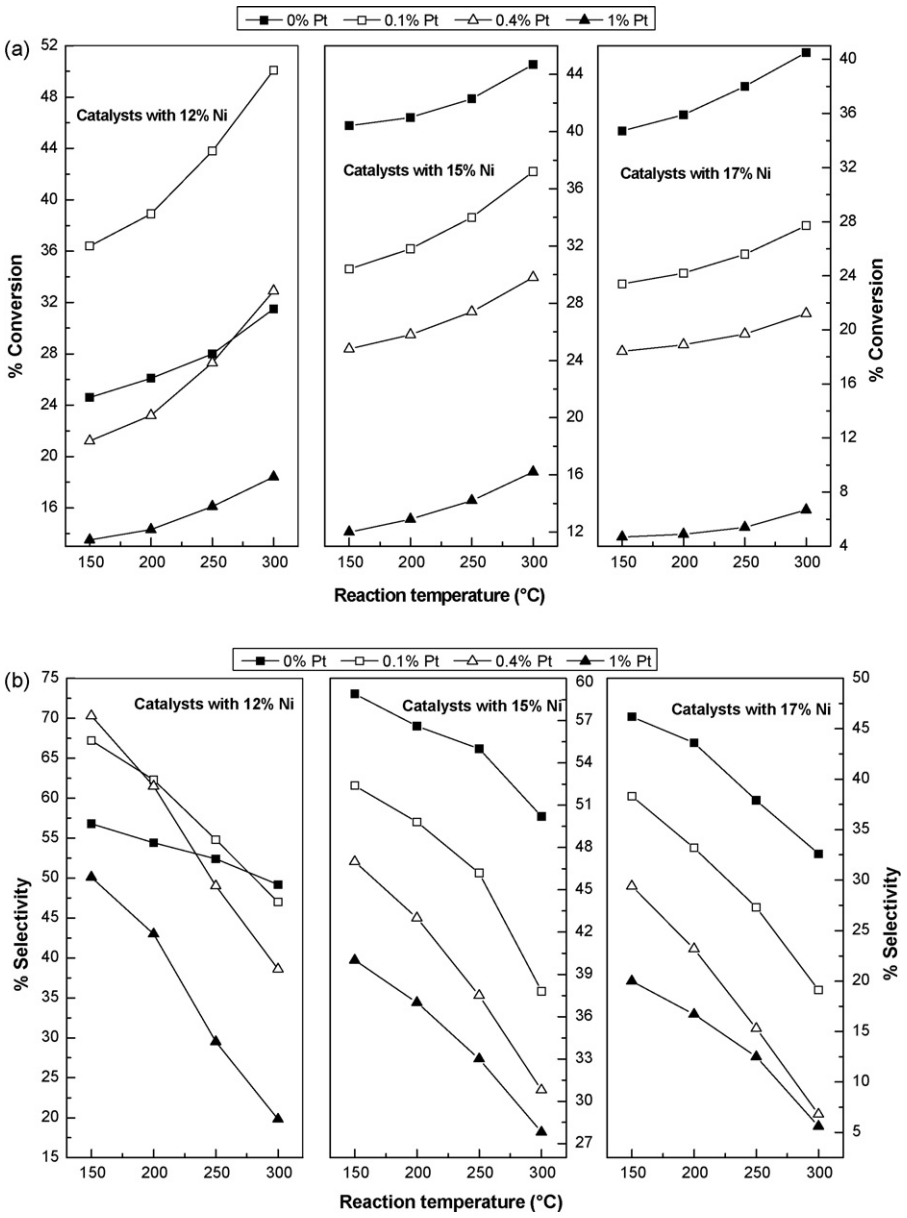


**Fig. 3.** (a) Effect of reaction temperature on conversion over $(Ni_xPt_y)_{AC}$ catalysts. Reaction conditions: TOS = 100 min, WHSV = 4 $h^{-1}$ and $H_2/n\text{-}C_{10}$(mol) = 5. (b) Effect of reaction temperature on isomerization selectivity over $(Ni_xPt_y)_{AC}$ catalysts. Reaction conditions: TOS = 100 min, WHSV = 4 $h^{-1}$ and $H_2/n\text{-}C_{10}$(mol) = 5.

from coke formation by catalyzing hydrogenation of coke precursors and by lowering Lewis acidity. It is known that Lewis sites catalyze favorably cracking reactions associated with the formation of coke [35,36]. Thus addition of platinum, which increase the surface protonic acidity of the samples, will be benefic in enhancing the catalysts stability.

### 3.3. Effect of reaction temperature

The conversion of *n*-decane and selectivity to isomerization as functions of the reaction temperature are presented in Fig. 3a and b (results were collected after reaching the steady state (TOS equal to 100 min on stream)). As should be expected, whatever the nickel and platinum contents, the reaction temperature has a great significance over the activity of these catalysts. The conversion of *n*-decane increased with an increment in reaction temperature, whereas the isomerization reaction decreased gradually (Fig. 3b) due to the consumption of isomerized products in consecutive hydrocracking. Same results were observed by Geng et al. [37] during their study on the hydroisomerization of *n*-tetradecane over Pt/SAPO-11 catalyst.

### 3.4. Choice of the optimal catalyst

Of the formulations screened in this work, $(Ni_{12}Pt_{0.1})_{AC}$ and $(Ni_{15}Pt_0)_{AC}$ catalysts showed by far the best performance. Thus it is interesting to study in more details these systems. Based on the conversion results, we could say that, regardless the reaction temperature, the $(Ni_{15}Pt_0)_{AC}$ sample display much higher catalytic activity as compared to $(Ni_{12}Pt_{0.1})_{AC}$ catalyst. These results may lead to wrong conclusion on the catalytic performance of the two systems, because in our case, we are more interested by the isomers yield than by the catalytic conversion. A close inspection of these two materials (Fig. 4) indicates that the $(Ni_{12}Pt_{0.1})_{AC}$ system displays higher isomers yields than the $(Ni_{15}Pt_0)_{AC}$ solid, whatever the reaction temperature, which means that the former sample is

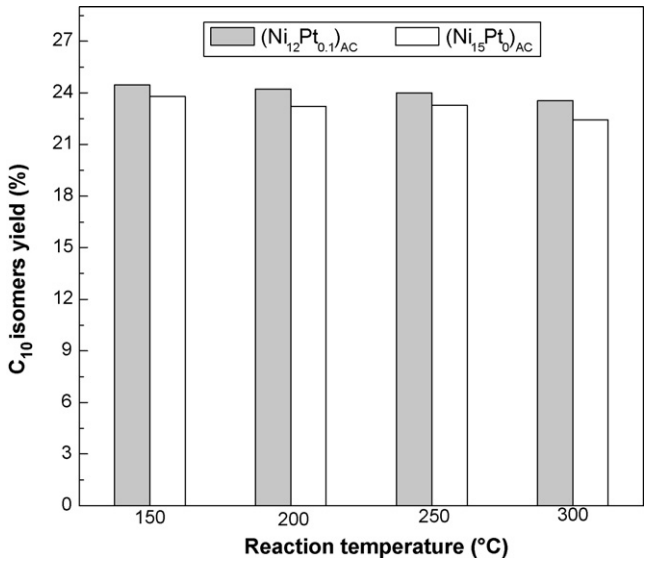


**Fig. 4.** $n$-$C_{10}$ isomers yield as a function of temperature over the $(Ni_{12}Pt_{0.1})_{AC}$ and $(Ni_{15}Pt_0)_{AC}$ catalysts at TOS = 100 min, WHSV = 4 $h^{-1}$ and $H_2/n$-$C_{10}$(mol) = 5.

more suitable than the latter one. Thus we will deal only with the former system in the following paragraphs.

As already mentioned, the catalytic conversion, in the case of the catalysts with 12% Ni, increased with platinum content to reach a maximum at about 0.1% Pt then it decreased monotonically for Pt concentration equal to 0.4%, which infers that the optimal platinum concentration should be ranged between 0.1% and 0.4%. To localize the most suitable platinum amount, two new catalysts containing the same nickel concentration (12%) and having 0.2 and 0.3 wt.% of platinum were synthesized using the same preparation protocol (mentioned in the catalysts preparation section). Then, the materials with 12% Ni were tested in the transformation of $n$-decane at different reaction temperatures and over a duration of 100 min. The collected data are displayed in Fig. 5, where it can be clearly seen that, regardless the Pt amount, a rise in the reaction temperature induces an increase in conversion, whereas the opposite behavior was observed for selectivity. Same results were reported in the case of $n$-hexadecane hydroisomerization over platinum-promoted tungstate-modified zirconia catalysts [38]. In addition, whatever the reaction temperature, with increasing platinum content, the conversion increased to reach a maximum at 0.3% Pt, and then decreased. The effect of the metal promotion was, however, more important in the case of catalysts with 0.2% Pt. On the other hand, selectivity to isomerization increased with platinum content to reach a maximum at about 0.3% platinum then it decreased monotonically. Such a catalytic behavior can be explained by the fact that in the range 0.1–0.3% platinum, the metallic sites of $(Ni_xPt_y)_{AC}$ catalysts are not sufficiently numerous for all the acid sites to be fed with intermediate alkenes, which means that the dehydrogenation of the reactant is the limiting step of the alkane transformation. Thus increased metal function of the catalysts (platinum) prompts the formation of isomers via a reduction of the diffusion path between two metallic sites. Hence, the possibility that the intermediate species would encounter acid sites and would be cracked during its migration from one metallic site to another is also less. In contrast, in the range 0.3–0.4% platinum, Pt sites are sufficiently numerous for all acid sites to be fed with intermediate alkenes and that the limiting step is the transformation of these alkenes on the acid sites, thus further increased metal function prevents the isomerization reaction and increases the rate of cracking and hydrogenolysis reactions (platinum is an active component for the hydrogenolysis reaction). Thus the observation of a maximum in the platinum content proves that, in our case, the reaction proceeds via a bifunctional mechanism.

Another point of view may be taken into account; additional protons can be generated on the surface by spillover of dissociated hydrogen atoms (formed on platinum sites) from platinum sites

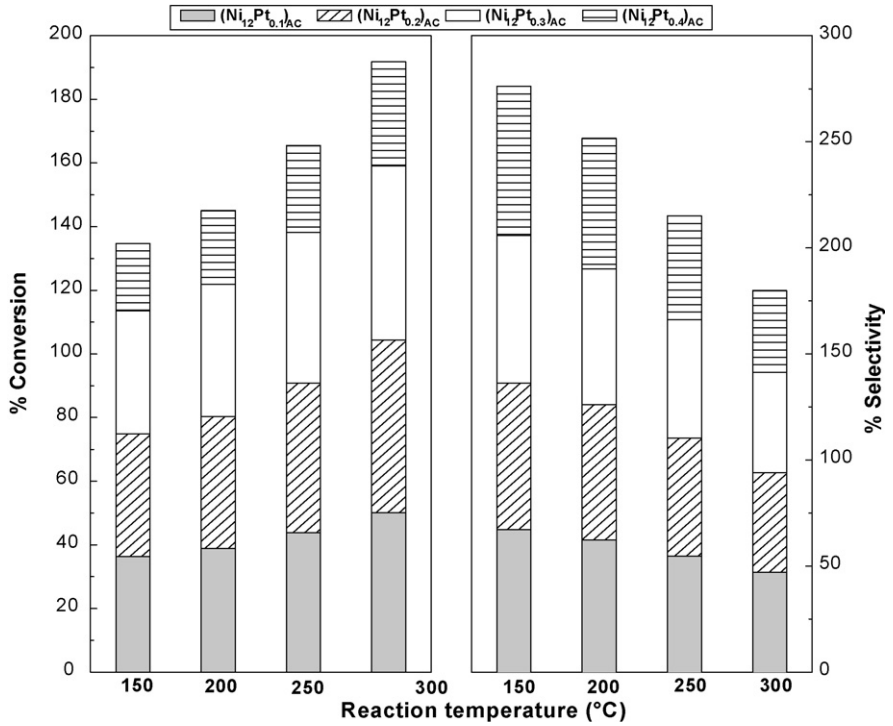


**Fig. 5.** Effect of reaction temperature on conversion and isomerization selectivity over $(Ni_{12}Pt_y)_{AC}$ catalysts. Reaction conditions: TOS = 100 min, WHSV = 4 $h^{-1}$ and $H_2/n$-$C_{10}$(mol) = 5.

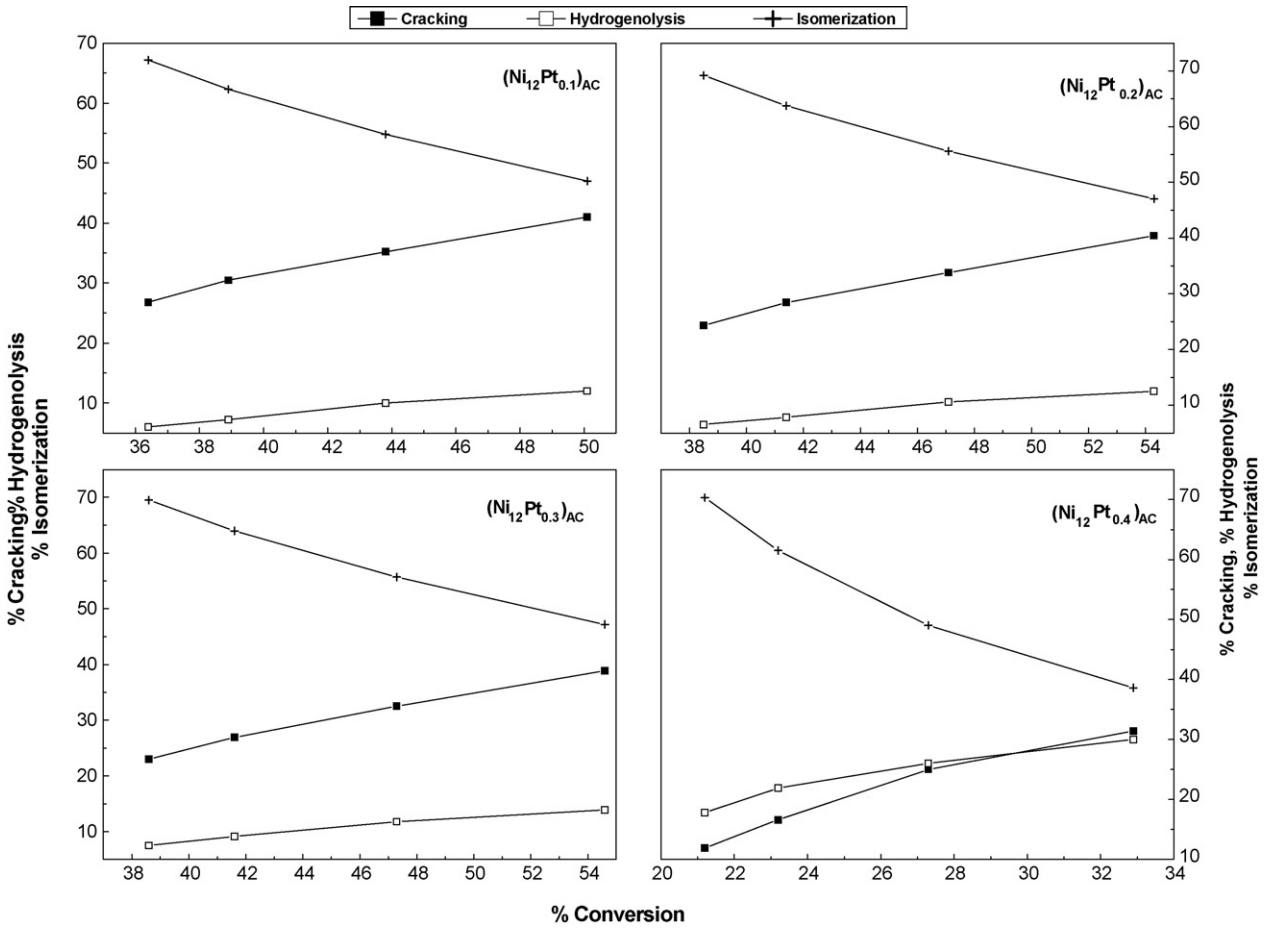


**Fig. 6.** Evolution of cracking, isomerization and hydrogenolysis reactions over $(Ni_{12}Pt_y)_{AC}$ catalysts as a function of conversion after 100 min on stream, at Reaction temperature ($T_R$) = 250 °C, WHSV = 4 $h^{-1}$ and $H_2/n\text{-}C_{10}$(mol) = 5.

followed by electron transfer from a spilled-over hydrogen atom to a Lewis acid site or to a second spilled-over hydrogen atom. The availability of the dissociated hydrogen is not only important for the generation of the acid sites but also for the elimination of ionic intermediates from the surface before β-scission events occur, avoiding cracking and polymerization reactions and thus increasing the isomerization selectivity.

The reaction pathways with respect to cracking, hydrogenolysis and isomerization were depicted in Fig. 6. Under our experimental conditions, $(Ni_{12}Pt_{0.1})_{AC}$ showed the highest cracking activity and $(Ni_{12}Pt_{0.4})_{AC}$ the lowest one, whereas the opposite behavior was observed for the hydrogenolysis reactions. Besides, $(Ni_{12}Pt_{0.3})_{AC}$ displayed the highest isomerization activity and $(Ni_{12}Pt_{0.4})_{AC}$ the lowest one. In addition, all catalysts showed virtually identical trends with increasing conversion in that the cracking and hydrogenolysis reactions increased monotonously at the expense of the decline of $C_{10}$ isomers. These results may be explained by the fact that cracking reaction, which being slower than the isomerization reaction is more favored at higher conversions. Besides, it is well known that in hydrocracking reactions branched products cannot be formed by secondary isomerization of the linear fragments [13,39] since competitive adsorption at the acid sites becomes less favorable with decreasing chain length of a fragment. These results verify that the formation of cracking products apparently succeeds the formation of branched isomers. On the other hand, the obtained results showed clearly that *n*-decane transformed on $(Ni_{12}Pt_x)_{AC}$ solids (where $x$ = 0.1–0.4) into isomerization products (monobranched (M) and multibranched (B)) and into cracked products (C) and that the product distribution depends on the catalyst and on the conversion. Fig. 7 shows that, on catalysts containing 0.2 and 0.3 wt.% platinum, only the monobranched isomers M appear as primary products, the B isomers being formed for conversions above 20% and the cracking products C for conversions above 10%. These results indicate that the reaction occurred mainly through a classical bifunctional mechanism. Same results were reported by Roussel et al. [40,41] during their study on the hydrocracking of *n*-decane over bifunctional sulfided NiW/silica–alumina catalyst and by Alvarez et al. [42] during their study on hydroisomerization and hydrocracking of *n*-decane over PtHY Catalysts. Besides, the collected data showed that cracking products, which were secondary products, became directly formed on the $Ni_{12}Pt_{0.4}$ catalyst, whereas cracking products as well as multibranched isomers are primary products on the $Ni_{12}Pt_{0.1}$ catalyst. These results imply that on this latter solid the metal-acid balance is shifted toward the acidic function so as the average distance between two platinum sites is great; the number of acid sites which can be encountered by the intermediate alkenes is therefore high, with consequently a high probability of several successive transformations of the alkene before hydrogenation on the acid sites. This explains why dibranched isomers and cracking products appear as primary products. In contrast in the case of $Ni_{12}Pt_{0.4}$ sample, the metal-acid balance is shifted toward the metallic function so as the cracking products are mainly formed via hydrogenolysis.

The evolution of the distribution of the methylnonane isomers, over the $(Ni_{12}Pt_x)_{AC}$ ($x$ = 0.1–0.4) catalysts, as a function of conversion is shown in Fig. 8. The distribution depend on the

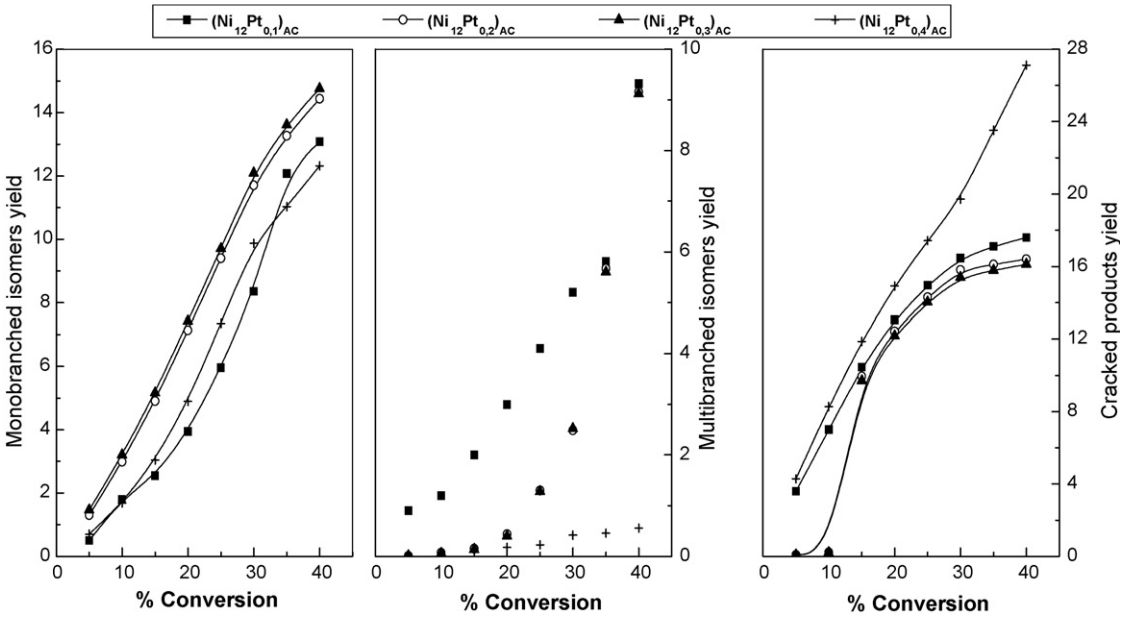


**Fig. 7.** Distribution of reaction products on $(Ni_{12}Pt_y)_{AC}$ catalysts as a function of conversion after 100 min on stream, at reaction temperature ($T_R$) = 250 °C, WHSV = 4 $h^{-1}$ and $H_2/n$-$C_{10}$(mol) = 5.

conversion of *n*-decane, the solids containing 0.1–0.3 wt.% platinum favored the formation of 3-methylnonane ($3MC_9$) and 4-methylnonane ($4MC_9$) over 2-methylnonane ($2MC_9$) and 5-methylnonane ($5MC_9$), whereas the $Ni_{12}Pt_{0.4}$ catalyst exhibited a lower selectivity toward $4MC_9$ as compared to the other methylnonanes. With increasing conversion, the $2MC_9$, $3MC_9$, and $4MC_9$ amounts present similar trends over all the catalysts, the yields of the two first methylnonanes increased with a rise in conversion, while the opposite trend is observed with the latter monobranched isomer. On the first three catalysts, $5MC_9$ decreased with increasing conversion, while it displayed a constant yield over the solid with 0.4 wt.% platinum.

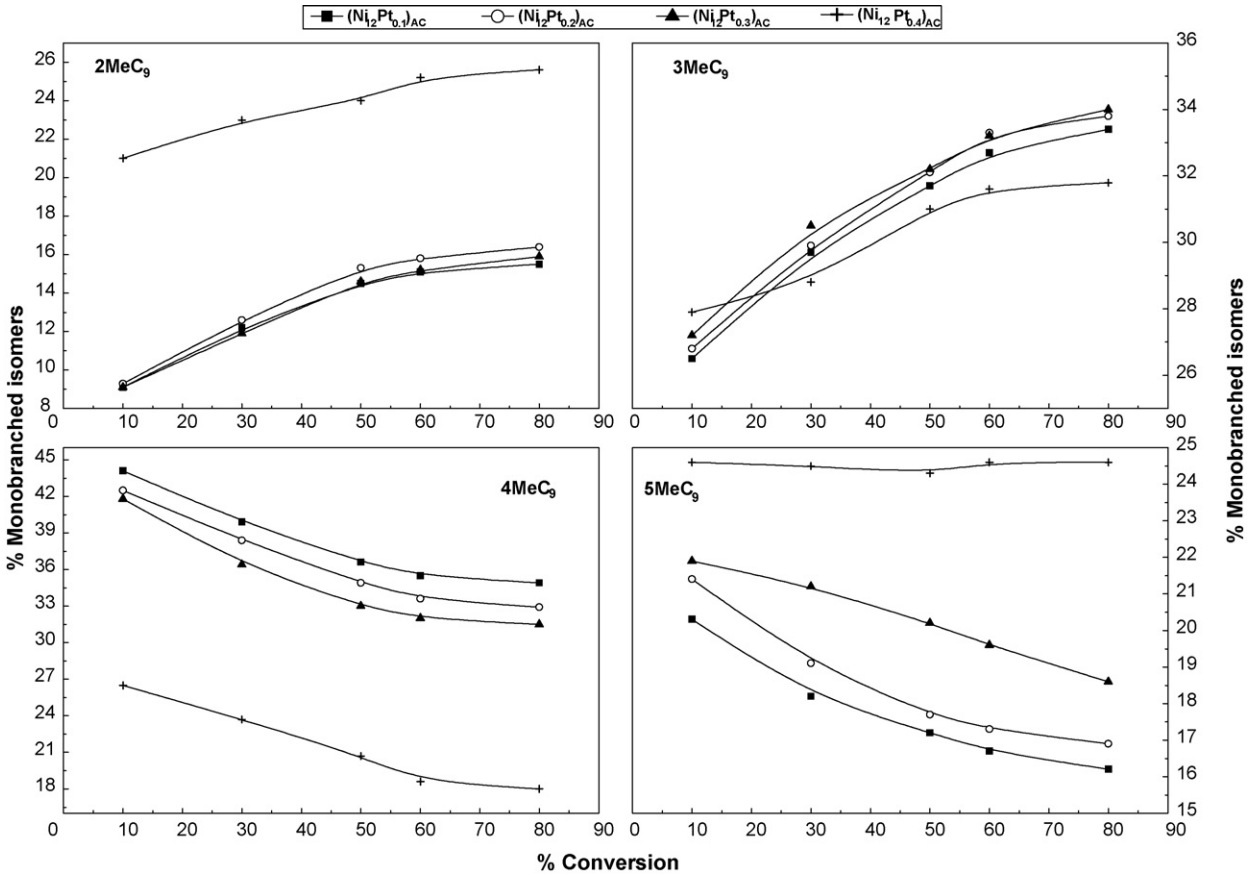


**Fig. 8.** Distribution of methylnonanes over $(Ni_{12}Pt_y)_{AC}$ catalysts at $T_R$ = 250 °C, TOS = 100 min, WHSV = 4 $h^{-1}$ and $H_2/n$-$C_{10}$(mol) = 5.

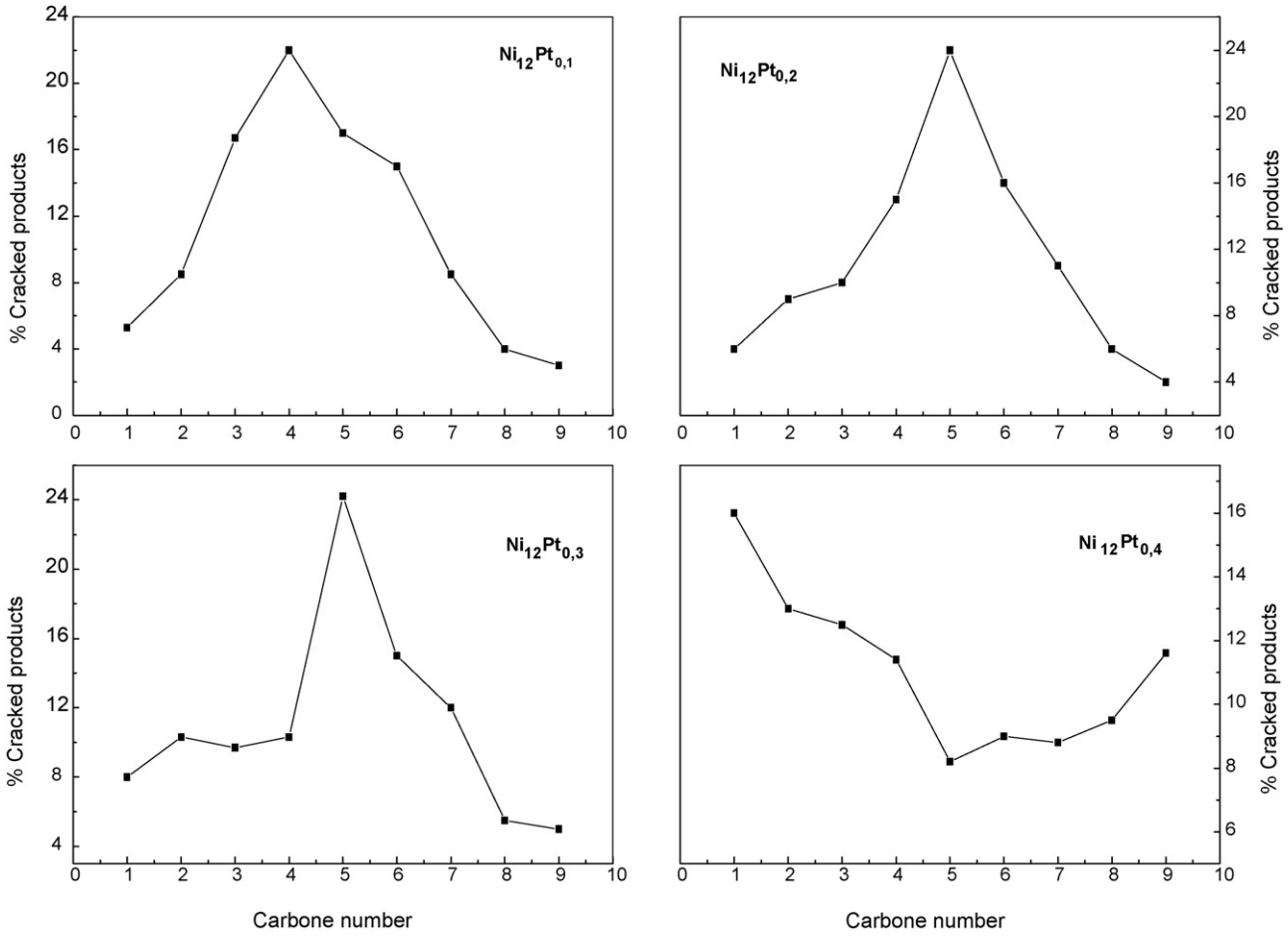


**Fig. 9.** Distribution of the cracked products over $(Ni_{12}Pt_y)_{AC}$ catalysts at 250 °C and a cracking yield of 25%. Reaction conditions: TOS = 100 min, WHSV = 4 $h^{-1}$ and $H_2/n$-$C_{10}$(mol) = 5.

The expected methylnonane proportion according to a protonated cyclopropane (PCP) mechanism is 1:2:2:1 for 2-, 3-, 4- and 5-methylnonane, respectively [39,43]. The experimental methylnonane isomer distribution obtained on $(Ni_{12}Pt_{0.1-0.3})_{AC}$ catalysts at high conversions of *n*-decane is close to that expected, so that when the reaction conditions are severe, it approaches the thermodynamic equilibrium. On $(Ni_{12}Pt_{0.4})_{AC}$, the initial content of 3- and 4-methylnonane is much lower, and that of 5-methylnonane much higher, as compared to the other solids.

The carbon number distributions of the hydrocracked products at a cracking yield of 25% are shown in Fig. 9. As can be seen, the carbon numbers of the cracked products range from $C_1$ to $C_9$ for all the catalysts, which suggests that hydrogenolysis interferes with cracking mechanism. $(Ni_{12}Pt_{0.2})_{AC}$ and $(Ni_{12}Pt_{0.3})_{AC}$ catalysts show maxima at $C_5$, while the distribution, over the $(Ni_{12}Pt_{0.1})_{AC}$ catalyst, was skewed toward $C_3$ and $C_4$ products because of secondary cracking of some of the $C_6$ and $C_7$ fragments (the balance metal-acid is less ideal [44]), similar results were reported by Galperin et al. [45] during their study on the hydroisomerization of *n*-decane over bifunctional Pt-MAPSO-31 catalysts, where they have mentioned that the existence of a maximum at $C_4$ could be considered as the evidence of a shift in the metal-acid balance, and by Elangovan and Hartmann [46] during their study on the isomerization of *n*-decane over Pt/MCM-41/MgAPO-n composite catalysts, where they have stated that secondary cracking is often observed over catalysts without well balanced acid and metal function. On the other hand, the $(Ni_{12}Pt_{0.4})_{AC}$ catalyst yields high amounts of $C_1$ and $C_9$ and shows a minimum at $C_5$ which suggests that hydrogenolysis plays an important role on this solid and that methylnonanes are cracked predominantly via the C-type cracking. The low selectivity of $C_5$ products is in agreement with the low content of 4-methylnonane in the isomers. According to [13,47,48], $C_5$ fragments could only be formed from 4-methylnon-6 cation; however, 4-methyl-6 cation formation is sterically restricted and corresponds to low 4-methylnonane selectivity, as was observed for $(Ni_{12}Pt_{0.4})_{AC}$.

Finally, it is noteworthy that for an ideal bifunctional catalyst, the carbon number distribution of the cracked products is symmetrical and the ratio of metal function to acidity (*n*(metal)/*n*(acid)) has an optimum value [49]. When the *n*(metal)/*n*(acid) is higher than the optimum value, hydrogenolysis reaction will be predominant. On the contrary, the consecutive cracking reaction will prevail. Therefore, it could be considered that the $(Ni_{12}Pt_{0.2})_{AC}$ was an ideal bifunctional catalyst for the *n*-decane hydroconversion.

## 4. Conclusions

In this paper we report a quantitative relationship between the activity, the stability, and the selectivity for *n*-decane hydroisomerization and hydrocracking on $(Ni_xPt_y)_{AC}$ catalysts and the metallic amount. The most outstanding observations are:

- Conversion decreased with TOS, the higher the activity showed by the catalyst, the more severe is its deactivation. Furthermore, medium acidity has been found to be of paramount importance

in activity decay because the strong acidity of the solids with 17% Ni appeared to be the main reason for the high coking forming propersity as compared to the samples with 15% Ni. On the other hand, the stronger deactivation of cracking reactions as compared to isomerization resulted in a net increase with TOS of decane isomers.

- Platinum induced a beneficial effect on the stability of the $(Ni_xPt_y)_{AC}$ solids by keeping the surface free from coke and by enhancing Brönsted acidity at the expense of Lewis acidity.
- The yield of branched isomers and the distribution of the methylnonane isomers, on the $(Ni_{12}Pt_{0.1-0.4})_{AC}$ catalysts, are found to be roughly a function of conversion. Besides, it was found that branching of *n*-decanes, over $(Ni_{12}Pt_{0.1-0.3})_{AC}$ samples, occurs mainly through protonated cyclopropane intermediates (PCP).
- For *n*-decane hydroconversion, the $(Ni_{12}Pt_{0.2})_{AC}$ catalyst gave a symmetrical carbon number distribution and a large amount of $C_5$ hydrocarbons in the cracked products due to its proper balance between metal and acid functions.

## References


[1] Y. Liu, C. Liu, Z. Tian, L. Lin, Energy Fuels 18 (2004) 1266–1271.
[2] M.D. Romero, A. de Lucas, J.A. Calles, A. Rodriguez, Appl. Catal. A 146 (1996) 425–441.
[3] N.Y. Chen, Oil Gas J. 75 (23) (1977) 165.
[4] T.R. Farrell, J.A. Zakarian, Oil Gas J. 84 (20) (1986) 47.
[5] J.A. Zakarian, R.J. Robson, T.R. Farrell, Eng. Prog. 7 (l) (1987) 59.
[6] A. Sequeira, in: J.J. McKetta (Ed.), Encyclopedia of Chemical Processing and Design, vol. 28, Marcel Dekker, New York, 1988, p. 347.
[7] R.J. Taylor, A.J. McCormack, Ind. Eng. Chem. Res. 31 (1992) 1731–1738.
[8] K.C. Park, S.K. Ihm, Appl. Catal. A 203 (2000) 201–209.
[9] J.M. Campelo, F. Lafont, J.M. Marinas, Appl. Catal. 170 (1998) 139–144.
[10] A. Corma, A. Martinez, S. Pergher, S. Peratello, C. Perego, G. Bellusi, Appl. Catal. 152 (1997) 107–125.
[11] S.J. Miller, Micropor. Mater. 2 (1994) 439–449.
[12] R.J. Taylor, R.H. Petty, Appl. Catal. 119 (1994) 121–138.
[13] R. Parton, L. Uytterhoeven, J.A. Martens, P.A. Jacobs, Appl. Catal. 76 (1991) 131–142.
[14] S. Zhang, Y. Zhang, J.W. Tierney, I. Wender, Fuel Proc. Technol. 69 (2001) 59–71.
[15] G.E. Glannetto, G.R. Perot, M.R. Guisnet, Ind. Eng. Chem. Prod. Res. Dev. 25 (1986) 481–490.
[16] V. Calemma, S. Peratello, C. Perego, Appl. Catal. 190 (2000) 207–218.
[17] J. Weitkamp, Ind. Eng. Chem. Prod. Res. Dev. 21 (1982) 550–558.
[18] M.J. Girgis, Y.P. Tsao, Ind. Eng. Chem. Res. 35 (1996) 386–396.
[19] S.J. Miller, Zeolites and related microporous materials: state of the art: 1994, in: p, in: J. Weitkamp, H.G. Karge, H. Pfeifer, W. Holderich (Eds.), Stud. Surf. Sci. Catal., vol. 84, Elsevier, Amsterdam, 1994, p. p2319.
[20] K. Tanabe, M. Itoh, K. Morishige, H. Hattori, Preparation of catalysts I, in: B. Delmon, P.A. Jacobs, G. Poncelet (Eds.), Stud. Surf. Sci. Catal., vol. 1, Elsevier, Amsterdam, 1976, p. 65.
[21] M. Hino, K. Arata, J. Am. Chem. Soc. 101 (1979) 6439–6441.
[22] J.C. Yori, J.C. Luy, J.M. Parera, Appl. Catal. 46 (1989) 103–112.
[23] M.C. Claude, G. Vanbutsele, J.A. Martens, J. Catal. 203 (2001) 213–231.
[24] S.J. Miller, Stud. Surf. Sci. Catal. 84 (1994) 2319.
[25] J.M. Campelo, F. Lafont, J.M. Marinas, J. Chem. Soc., Faraday Trans. 91 (1995) 1551.
[26] P. Mériaudeau, V.A. Tuan, V.T. Nghiem, S.Y. Lai, L.N. Hung, C. Naccache, J. Catal. 169 (1997) 55–66.
[27] A.K. Sinha, S. Sivasanker, P. Ratnasamy, Ind. Eng. Chem. Res. 37 (1998) 2208–2214.
[28] Z. Wang, Z. Tian, F. Teng, G. Wen, Y. Xu, Z. Xu, L. Lin, Catal. Lett. 103 (2005) 109–116.
[29] Y. Rezgui, M. Guemini, Appl. Catal. 282 (2005) 45–53.
[30] Y. Rezgui, M. Guemini, Appl. Catal. 335 (2008) 103–111.
[31] M. Guemini, Y. Rezgui, Appl. Catal. 345 (2008) 164–175.
[32] Y. Rezgui, M. Guemini, A. Tighezza, A. Bouchemma, Catal. Lett. 87 (2003) 11–24.
[33] J.M. Grau, V.M. Benitez, J.C. Yori, C.R. Vera, J.F. Padilha, L.A.M. Pontes, A.O.S. Silva, Energy Fuels 21 (2007) 1390–1395.
[34] M.G. Falco, S.A. Canavese, R.A. Comelli, N.S. Figoli, Appl. Catal. 201 (2000) 37–43.
[35] S. Arenamnarta, W. Trakarnpruk, Int. J. Appl. Sci. Eng. 4 (2006) 21–32.
[36] C.D. Chang, C.T.-W. Chu, R.F. Socha, J. Catal. 86 (1984) 289–296.
[37] C.H. Geng, F. Zhang, Z.X. Gao, L.F. Zhao, J.L. Zhou, Catal. Today 93–95 (2004) 485–491.
[38] S. Zhang, Y. Zhang, J.W. Tierney, I. Wender, Appl. Catal. 193 (2000) 155–171.
[39] J.A. Martens, P.A. Jacobs, Zeolites 6 (1986) 334–348.
[40] M. Roussel, J.-L. Lemberton, M. Guisnet, T. Cseri, E. Benazzi, J. Catal. 218 (2003) 427–437.
[41] M. Roussel, S. Norsic, J.-L. Lemberton, M. Guisnet, T. Cseri, E. Benazzi, Appl. Catal. 279 (2005) 53–58.
[42] F. Alvarez, F.R. Ribeiro, G. Perot, C. Thomazeau, M. Guisnet, J. Catal. 162 (1996) 179–189.
[43] J.M. Campelo, F. Lafont, J.M. Marinas, React. Kinet. Catal. Lett. 62 (1997) 371–376.
[44] A. Aerts, A. van Isacker, W. Huybrechts, S.P.B. Kremer, C.E.A. Kirschhock, F. Collignon, K. Houthoofd, J.F.M. Denayer, G.V. Baron, G.B. Marin, P.A. Jacobs, J.A. Martens, Appl. Catal. 257 (2004) 7–17.
[45] L.B. Galperin, S.A. Bradley, T.M. Mezza, Appl. Catal. 219 (2001) 79–88.
[46] S.P. Elangovan, M. Hartmann, J. Catal. 217 (2003) 388–395.
[47] P.A. Jacobs, M.A. Martens, J. Weitkamp, H.K. Beyer, Faraday Discuss. Chem. Soc. 72 (1981) 353–369.
[48] L.B. Galperin, Appl. Catal. 209 (2001) 257–268.
[49] K. Fang, W. Wei, J. Ren, Y. Sun, Catal. Lett. 93 (2004) 235–242.